Call: HORIZON-CL5-2021-D5-01

Hyperconnected simulation ecosystem supporting probabilistic design and predictive manufacturing of next generation aircraft structures

CAELESTIS

Deliverable D4.1

AFP Process Interoperable Digital Twin with permeability predictions

Work Package 4

Digital manufacturing and defects prediction

Document type	:	Report
Version	:	1.0
Date of issue	:	30/04/2024
Dissemination level	:	PUBLIC
Lead beneficiary	:	ADD

Funded by the European Union. Views and opinions expressed are however those of the author(s) only and do not necessarily reflect those of the European Union or [EUROPEAN CLIMATE, INFRASTRUCTURE AND ENVIRONMENT EXECUTIVE AGENCY (CINEA)]. Neither the European Union nor the granting authority can be held responsible for them.

Funded by the European Union

Funded by the European Union

Executive Summary

Abstract	This report presents the progress made in developing advanced simulation capabilities for the Automated Fiber Placement (AFP) and Resin Transfer Molding (RTM) processes, as part of the CAELESTIS project. Key achievements include integrating defect generation probabilities into the AFP process simulation using ADDPath® software, developing an automated workflow to generate permeability Reduced Order Models (ROMs) for RTM simulations, and creating methods to generate synthetic gap and misalignment defect data based on real point cloud data distributions. The report also outlines the data flow and simulation strategies employed. Preliminary results are presented, showcasing the initial stage leading to final simulations on the Fan Outlet Guide Vane (FOGV) use case. Future work will focus on integrating experimental defect data, completing permeability ROM training and validation, exploring additional defect types for synthetic data generation, and conducting refined simulations to enable parametric studies for optimizing the final FOGV design.
Keywords	Automated Fiber Placement (AFP), Resin Transfer Molding (RTM), process simulation, defect modeling, permeability, Reduced Order Models (ROMs), synthetic defect data, point cloud processing

Funded by the European Union

Revision history

Version	Author(s)	Changes	Date
0.1	Francisco Serrano (ITA)	Table of Contents (proposal)	01/04/2024
0.2	Pravin Luthada (ADD)	Content	02/08/2024
0.3	Francisco Serrano (ITA) Carlos Magdalena (ITA) Ricardo Teruel (ITA)	Section 4 and 5	08/04/2024
0.4	Pravin Luthada (ADD)	Section 1 and 3	10/04/2024
0.5	Pravin Luthada (ADD)	Formating and printing	12/04/2024
0.6	Pravin Luthada (ADD)	JVN and Veronica comments	26/04/2024
0.7	Pravin Luthada (ADD)	Printing revision	30/04/2024
1.0	Pravin Luthada (ADD)	Submitted	30/04/2024

Funded by the European Union

LIST OF FIGURE

FIGURE 2.1 NUMERICAL WORKFLOW FOR PROCESSES DIGITAL TWINS 9
FIGURE 2.2 NUMERICAL AND PHYSICAL DATA EXCHANGED BETWEEN ADDPATH®, PERMEABILITY ROM AND PAM-RTM® 11
FIGURE 3.1 LAYUP AND BOUNDARY SURFACES OF POC2 14
FIGURE 3.2 LAMINATE CONFIGURATION GENERATION GUI 15
FIGURE 3.3 PLY CONFIGURATION GENERATION GUI 16
FIGURE 3.4 PLY DROP-OFFS IN FLAT PLAT LAMINATE WITH DIFFERENT ORIENTATION 20
FIGURE 4.1: WORKFLOW DEVELOPED TO GENERATE PERMEABILITY ROM. 25
FIGURE 4.2: EXAMPLE OF AN RVE CONSISTING OF 5 LAYERS ARRANGED AS 0/90/0/90/0 WITH OVERLAP DEFECT. AN INNER VOLUME IS HIGHLIGHTED AS A DEMONSTRATOR. 26
FIGURE 4.3 TRADITIONAL WOVEN FABRIC GENERATED USING TEXGEN. 27
FIGURE 4.4 GEOMETRY GENERATED USING IN-HOUSE PYTHON SCRIPT + TEXGEN'S LIBRARIES. 27
FIGURE 4.5 WOVEN TEXTILE AND ITS NODES AND PATHS. 28
FIGURE 4.6 TEXGEN REPRESENTATION OF AFP DEFECTS AND A MESH GENERATED. 29
FIGURE 4.7 TOW WITH NO DEFECTS GENERATED BY RECTANGULAR SECTION. 30
FIGURE 4.8 TOW WITH DEFECT GENERATED BY SECTION POINTS. 31
FIGURE 4.9 MESH GENERATED BY THE IN-HOUSE PYTHON SCRIPT. 31
FIGURE 4.10 TOW GEOMETRY PROVIDED BY THE CASE GENERATOR. 32
FIGURE 4.11 OVERLAP (TOP) AND GAP (BOTTOM) GENERATED BY THE IN-HOUSE PYTHON SCRIPT. ORANGE TOW IS THE WRONGLY POSITIONED. 32
FIGURE 4.12 A REPRESENTS THE OVERLAYED TOW AND B THE GAP GENERATED BECAUSE OF THE MISPLACED TOW (OVERLAP SITUATION). ORANGE IS THE FIRST TOWS ALLOCATED AND GREEN THE SECOND. 33
FIGURE 4.13 A REPRESENTS THE GAP LEFT BY THE AFP AND B THE CONSEQUENCE (GAP SITUATION). ORANGE IS THE FIRST TOW ALLOCATED AND GREEN THE SECOND. 33
FIGURE 4.14 REPRESENTATION OF THE TRANSITION ZONES. TOWS BELONGING TO THE SAME LAYER HAVE THE SAME COLOR. 34
FIGURE 4.15 REPRESENTATION OF THE STACKING OF THE TOWS WITH A DEFECT. TOWS BELONGING TO THE SAME LAYER HAVE THE SAME COLOR. 34
FIGURE 4.16: RVE GEOMETRY. 36
FIGURE 4.17: DIFFERENT PACKING ARRANGEMENTS: A1) QUADRILATERAL PACKING FOR A GIVEN FVF, A2) QUADRILATERAL ARRANGEMENT FOR MAXIMUM FVF, B1) HEXAGONAL ARRANGEMENT FOR A GIVEN FVF, AND B2) HEXAGONAL ARRANGEMENT FOR MAXIMUM FVF. 38
FIGURE 4.18: GEBART'S PERMEABILITY DEPENDING ON THE FIBER VOLUME FRACTION. 39
FIGURE 4.19 CFD SIMULATION: A) GEOMETRY OF AN RVE WITH OVERLAP, AND B) VELOCITY ARROWS FROM CFD RESULTS. 41
FIGURE 4.20 EXAMPLE OF AREAS OF INFLUENCE OF AN OVERLAP (RED) AND GAPS (GREEN) SOME POSSIBLE SETS ARE HIGHLIGHTED IN MAROON, FROM LEFT TO RIGHT THERE WOULD BE TWO SETS THAT BELONG TO THE OVERLAP CASE, A SET THAT HAS NO DEFECT AND TWO SETS THAT BELONG TO THE GAP CASE. 43
FIGURE 4.21 REPRESENTATION OF THE CONTRIBUTION OF 3 VARIABLES APPROXIMATED TO THE 3RD ORDER. 45
FIGURE 4.23 POINT CLOUD FOR A REAL TAPE DEPOSITION 47
FIGURE 4.24 CLEANED IMAGE BY USING IQR 48
FIGURE 4.25 SEGMENTED IMAGE 48
FIGURE 4.26 SYNTHETIC DATA DISTRIBUTION 49
FIGURE 4.27 SYNTHETIC GAP GENERATION 49
FIGURE 4.28 TAPE MISALIGNMENT 50
FIGURE 4.29 MISALIGNMENT EVOLUTION 51

Funded by the European Union

LIST OF TABLE

TABLE 1 EXAMPLE OF THE DATA SHARED INITIALLY IN THE TXT FILE 11
TABLE 2 EXAMPLE OF THE DATA ADDED FROM ADDPATH® SIMULATION TO THE TXT FILE 11
TABLE 3 EXAMPLE OF THE LPERM FILE UPDATED WITH PERMEABILITY INFORMATION OF EACH PAM-RTM® ELEMENT. 11
TABLE 4 EXAMPLE OF ELEMENT ID AND CENTROID X Y Z COORDINATES. 13

Funded by the European Union

TABLE OF CONTENTS

1 INTRODUCTION 7
2 AFP DIGITAL TWIN IN THE GLOBAL WORKFLOW 9
3 AFP SIMULATIONS (ADD) 13

3.1 Data inflow 13

3.1.1 Layup surface 14
3.1.2 Process Parametrization for AFP Planning 14
3.1.3 Defects 17

3.2 Strategy and trajectory planning 18

3.3 Planning strategy 19

3.3.1 Ply drop-offs 19

3.4 Tow generation and defect identification 21

3.4.1 Tape geometry generation 21
3.4.2 Defect identification 21

3.5 Ready and output data for PAMRTM 21

3.5.1 Centroid data update 21
3.5.2 Terminology 22

4 PERMEABILITY SURROGATE GENERATION (ITA) 23

4.1 RVE generation 26

4.2 Case configuration 34

4.3 Postprocessing 39

4.4 Surrogate training 42

4.5 AFP-RTM connection and permeability surrogate assessment 45

4.6 Synthetic Data generation for Defect detection models trainning 47

5 CONCLUSION AND FUTURE WORK 52

Funded by the European Union

1 INTRODUCTION

The aim of the CAELESTIS project is to create an innovative, comprehensive Interoperable Simulation Ecosystem (ISE) that seamlessly integrates product design, distributed engineering teams (DET), and manufacturing specialists. This ecosystem seeks to expedite the design and engineering refinement of groundbreaking aircraft for the future. A pivotal aspect of CAELESTIS is its provision of high-fidelity, model-based digital twins, enabling precise predictions at various stages of the product development cycle. This cycle encompasses processes such as automated fiber placement (AFP), laser powder bed fusion (L-PBF), resin transfer molding (RTM), component assembly, and mechanical assessments to determine the product's structural performance.

Within the context of manufacturing processes, there is a pressing need not only to minimize uncertainties at each stage and reduce the number of defective parts but also to guide the design of new components with a holistic focus on both manufacturing and mechanical performance throughout all stages. Consequently, the initial phases of design and manufacturing are expedited in pursuit of a component that considers all mechanical and manufacturing requirements, including the unavoidable defects that may arise during various stages such as AFP, L-PBF, RTM, assembly, and mechanical testing. This acceleration is made feasible through the execution of extensive simulation campaigns, involving a multitude of design and manufacturing scenarios across the entire chain of manufacturing and mechanical performance. Utilizing High-Performance Computing (HPC) resources enables realistic time scales, providing faster and more accurate insights for optimizing both product and process within the manufacturing chain. This approach delivers rapid and precise predictive insights across various design and manufacturing scenarios, offering a comprehensive array of outputs related to mechanical performance, manufacturability, sensitivity analysis and uncertainty quantification.

This deliverable specifically focuses on the AFP, RTM, and L-PBF Digital Twins employed in the CAELESTIS project for manufacturing simulations. The modeling strategy for each stage, along with the overarching workflow of the manufacturing chain developed in the CAELESTIS use case (fan outlet guide vane (FOGV)), is elucidated. Importantly, this modeling strategy is not

Funded by the European Union

limited to simulating the FOGV but is also applicable to any component manufactured using AFP, L-PBF, and RTM processes.

The deliverable elaborates on the AFP process simulations, which are often limited to trajectory planning for given material, parameters, and layup surface. The proposed work utilizes the simulation software ADDPath® to integrate defect generation probabilities, such as misalignment, gaps, and overlaps. The probabilities are presently randomized, and at a later stage, the defect probabilities will be generated based on experimental defect classification from defects measured by machine vision. The AFP process simulation based on randomized defects allows for the completion of the workflow process for the permeability surrogate model and provides information for RTM modeling and simulation.

Furthermore, the deliverable discusses the innovative model developed to specifically predict permeability in AFP materials. This model leverages integrated simulations of AFP and RTM processes to capture the complex interplay between material properties, manufacturing parameters, and permeability. The workflow developed to generate the permeability Reduced Order Models (ROMs) is presented, along with the data generation, model training, preprocessing for CFD simulations, CFD simulation, and postprocessing of the simulations.

The deliverable also includes the L-PBF analysis of the metallic insert located at the ends of the FOGV, starting with the original design that does not initially leverage the benefits of the PBF process. RTM process models are explained from input data through filling, curing, and distortion analysis, showing preliminary results as a demonstrator.

Therefore, this deliverable is structured as follows: Section 2 outlines the overall workflow of the CAELESTIS simulations and contextualizes the AFP, RTM, and L-PBF processes within this framework; Section 3 presents the AFP simulations and the integration of defect generation probabilities; Section 4 describes the permeability surrogate model for AFP materials; Section 5 summarizes the conclusions and outlines future work to be developed during the extension of work package 4.

Funded by the European Union

2 AFP DIGITAL TWIN IN THE GLOBAL WORKFLOW

The AFP digital twin plays a crucial role in the global workflow of the CAELESTIS project, serving as a key component in the simulation and optimization of the manufacturing process for composite components such as the fan outlet guide vane (FOGV). The AFP process simulation, performed using the ADDPath® software, is integrated into a comprehensive workflow that encompasses various stages, including permeability predictions, resin transfer molding (RTM) simulations, and laser powder bed fusion (L-PBF) simulations for metallic inserts.

Workflow description focusing on AFP process and permeability predictions, including links between software for AFP process and other software (RTM). The global processes workflow defined and built in the WP4 is illustrated in Figure 2.1.

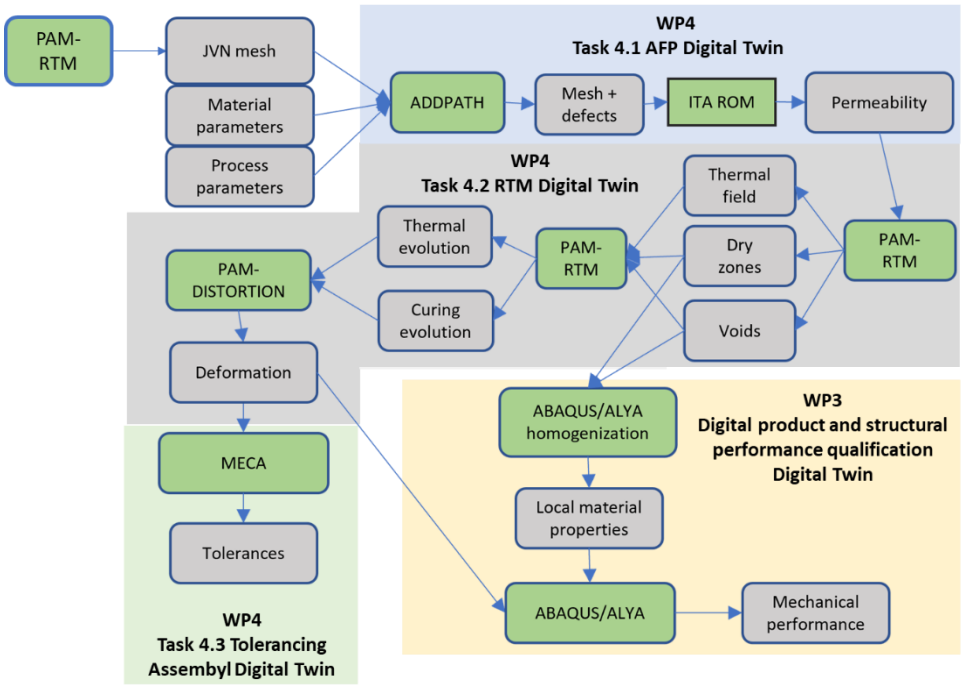

Figure 2.1 Numerical workflow for processes digital twins

Funded by the European Union

Two of main objectives of CAELESTIS project are:

- to develop a numerical workflow between processes digital twins,
- to propagate processes defects in the numerical workflow.

To build the numerical workflow between the different digital twins dedicated to each process of the manufacturing of the complete OGV, with the exchange of numerical and physical data, as input / output parameters, Python® scripts and intern development in some software have been developed, based and using the API of the different software.

For the workflow between AFP and RTM processes simulations, two dedicated numerical files, the lperm file and a txt file, have been created, which will be used and completed at each step of the digital thread. The steps are shown in Figure 2.1 and detailed in the following points:

- 1° initial generation of the lperm file, by PAM-RTM® with the meshing data,
- 2° calculation of the centroid of each finite element of the meshing, with its coordinates with Python® script and integration of the data in the txt file. shows an example of the initial data of the txt file,
- 3° integration of the orientation and the local reference axes data for each ply of the preform at the centroid location, coming from ADDPath®, and integration of data in the txt file,
- 4° integration of the potential AFP process defects, misalignments, gaps and/or overlaps data for each ply of the preform, with the locations and the dimensions of the defects, at the centroid location, coming from ADDPath®, and integration of data in the txt file. Table 2 shows an example of the updated data of the txt file,
- 5° evaluation of the data from txt file and integration of the permeabilities values, coming from surrogate model, with defects consideration, and integration of data in the lperm file,
- 6° the completed lperm file, with all the previous information is the used in PAM-RTM® for the filling simulation. The effect of the occurrence of defects in the preform is considered by the variations of the permeabilities values. Table 3 shows an example of the final lperm file.

Funded by the European Union

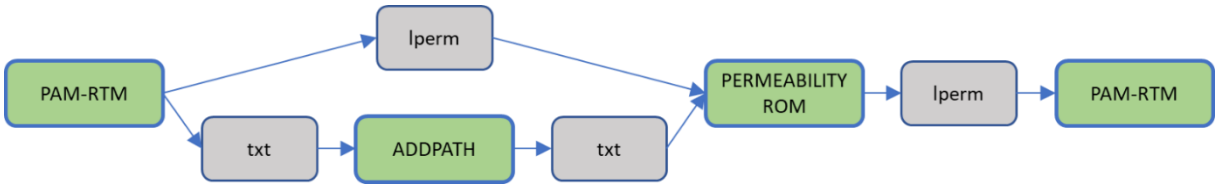

Figure 2.2 Numerical and physical data exchanged between ADDPath®, permeability ROM and PAM-RTM®

ID	Coordinates		
3457	147.5	77.5	1.95
3458	150.0	77.5	1.85
…	…	…	…

Table 1 Example of the data shared initially in the txt file

Layer Number	Ply Orientation	Normal	0º Layer Orientation	Distance	
1	0,0,0,0,0,0,0,0,0,0	0,0,-1	1,0,0	1.95	
1	0,0,0,0,0,0,0,0,0,0	0,0,-1	1,0,0	1.85	
…	…	…	…	…	
Gap	**Gap Distance**	**Gap Size**	**Overlap**	**Overlap Distance**	**Overlap Size**
-1	9999	9999	-1	9999	9999
-1	9999	9999	-1	9999	9999
…	…	…	…	…	…

Table 2 Example of the data added from ADDPath® simulation to the txt file

ID	Thickness	Fiber Content	K1	K2	K3
3457	0.00018	0.55	1.42e-09	5.75e-13	6.04e-13
3458	0.00018	0.55	1.42e-09	5.75e-13	6.04e-13
…	…	…	…		…
Perm_Vec1_x	**Perm_Vec1_y**	**Perm_Vec1_z**	**Perm_Vec2_x**	**Perm_Vec2_y**	**Perm_Vec2_z**
0	1	0	0.9368	0	-0.3498
0	1	0	0.93413	0	-0.3376
…	…	…	…		…

Table 3 Example of the lperm file updated with permeability information of each PAM-RTM® element.

The workflow begins with the generation of the layup and boundary surface files, which define the area for fiber placement and any adjacent surfaces for potential overflowing. These files serve as inputs to the ADDPath® software. Additionally, the meshing data generated by PAM-RTM® is processed using a Python® script to calculate the centroid of each finite element, providing crucial input for the AFP simulation.

Funded by the European Union

Within ADDPath®, the process parameters for AFP planning are defined, including laminate and ply definitions. The laminate definition encompasses tow width, tow thickness, areal density, minimum cut length (MCL) extension, and the global reference for ply angles. The ply definition includes ply number, angle, gaps, manufacturing excess, staggering, coverage, and MCL extension. The simulation also incorporates the generation of defects such as misalignment, gaps, and overlaps, which are currently randomized but will be based on experimental defect classification from machine vision data in the future.

The AFP simulation in ADDPath® generates detailed information about the fiber placement process, including the exact geometry of each tape for each ply and pass, as well as the identification of defects. This information is then used to update the centroid data, which includes the ply orientation, normal vector, 0-degree layer orientation, and distance from the layup surface for each point. Additionally, the presence and characteristics of gap and overlap defects are determined for each centroid point.

The updated centroid data, along with the defect information, is then utilized to generate a permeability surrogate model using computational fluid dynamics (CFD) simulations and the ALYA® software. The surrogate model captures the complex interplay between material properties, manufacturing parameters, and permeability, taking into account the presence of defects. The generated permeability data is then integrated back into the workflow, serving as input for the PAM-RTM® software to simulate the resin transfer molding process.

Furthermore, the AFP digital twin provides crucial information for the L-PBF simulations of the metallic inserts located at the ends of the FOGV. The design of these inserts can be optimized based on the results of the AFP simulation, ensuring compatibility and optimal performance of the final composite component.

Throughout the workflow, data is exchanged between the various software tools using specifically designed file formats, such as the lperm file, which contains information about the mesh, centroid coordinates, ply orientations, defects, and permeability values. This file serves as a critical link between the AFP simulation (ADDPath®), permeability prediction (ALYA®), and RTM simulation (PAM-RTM®).

Funded by the European Union

3 AFP SIMULATIONS (ADD)

AFP process simulations often are limited to trajectory planning for a given material, parameters and layup surface. However, such simulations are only useful for robot language program generation and do not have a way to identify, communicate defects in the process chain. The proposed work the simulation software ADDPath® to integrate defect generation probabilities e.g. misalignment, gaps, overlaps; The probabilities are presently randomised and at a later stage the defect probabilities will be generated based on experimental defect classification (ESI using topology data analysis, TDA) from defects measured by machine vision (T6.1). The AFP process simulation based on randomised defects allow us to complete the workflow process for Permeability surrogate model and ready information for RTM modelling and simulation. To initiate the AddPath workflow please refere to the D2.2 Execution of External Deployed Software: ADDPath Execution.

3.1 Data inflow

To initiate the process of simulation with ADDpath it needs to be prompted with input. During the project a detailed strategy to ensuring the data input from other software's in the simulation workflows can be read.

Centroids: As shown in the Figure 2.1 the workflow begins at initial generation of the file, by PAM-RTM® with the meshing data. The mesha data is than passed through a Python® script for calculation of the centroid of each finite element mesh. The generated file snapshot is given below Table 4

Element ID	*X (mm)*	*Y(mm)*	*Z(mm)*
5460	*150.00.00*	*72.49999999999999*	*1.9499999999999997*
5461	*152.05.00*	*74.99999999999999*	*1.8499999999999999*
5462	*152.05.00*	*72.49999999999999*	*1.09*
5463	*147.05.00*	*67.49999999999999*	*1.9499999999999997*
5464	*150.00.00*	*67.49999999999999*	*1.8499999999999999*
5465	*147.05.00*	*64.99999999999999*	*1.09*

Table 4 Example of Element ID and Centroid X Y Z coordinates.

Funded by the European Union

3.1.1 Layup surface

Layup and Boundary Surface Files

The layup surface defined as the area onto which the intended fibre placement can be carried out by definition. The boundary surface is defined as surface that is a continuous surface adjacent to layup surface and allows for any unintended or overflowing fibre placement to be carried out. Both the surface files can are a onetime input into the simulation and are provided by the end user as a definition of the layup. An example of POC2 layup and boundary surfaces are as shown in Figure 3.1

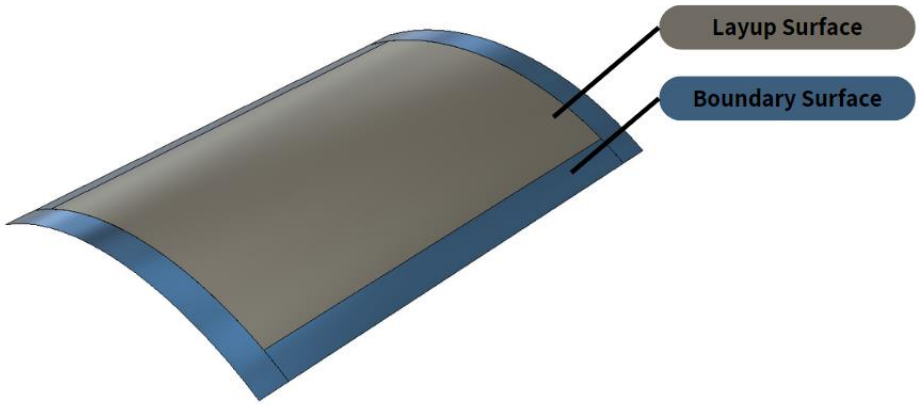

Figure 3.1 Layup and boundary surfaces of POC2

3.1.2 Process Parametrization for AFP Planning

Process Parameter for AFP planning are divided into two main categories i.e. Laminate definition and Ply definition. To define the process parameter the end user is provided with simple user interface where they could input the relevant details.

Laminate definition

The laminate definition (Figure 3.2) in the context of CAELESTIS is includes the following parameters.

Funded by the European Union

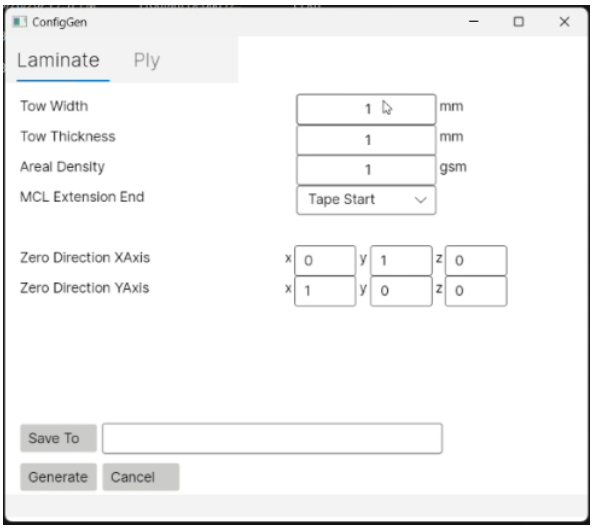

Figure 3.2 Laminate configuration generation GUI

- Tow Width: The width of the tape used in the AFP process.
- Tow Thickness: The compacted thickness i.e. post layup thickness, of the tape.
- Areal density: Area weight of tape in grams per square meters.
- MCL Extension End: Minimum Cut Length (MCL) is a limitation of the AFP process mechanics that limits the minimum length of the tape that can be placed. This MCL is usually visible on the corners of laminate where smaller piece of tape needs to be placed. The option in the configuration allows for controlling the excess material layup on either tape start, end or equally divided on either side.
- Zero Direction XAxis and YAxis: As for all composites laminate a global reference with respect to which ply angles are measured. The definition requires a vector defining the 0 degree direction and perpendicular vector i.e. Zero Direction Y axis, defining the 90 degree direction.

Funded by the European Union

Ply definition

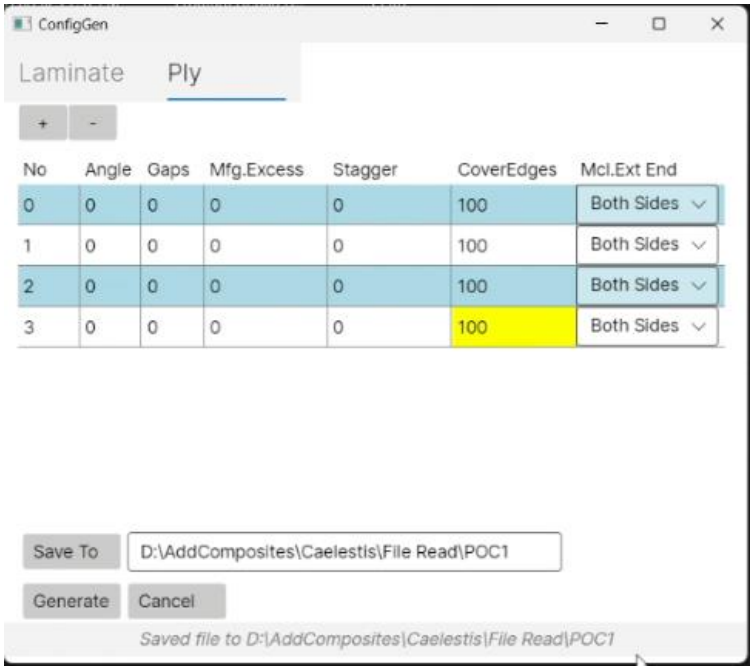

Figure 3.3 Ply configuration generation GUI

In ADDPath®, the definition of a ply for an AFP process involves several parameters that can be specified using the configuration generator shown in the Figure 3.3. The main parameters include:

- Ply Number: The unique identifier for each ply in the laminate.
- Angle: The orientation of the fibers within the ply, measured with respect to the global 0-degree direction.
- Gaps: The spacing between the tows or tapes, which can be set to zero for no gaps or a positive value to introduce gaps intentionally.
- Manufacturing Excess: Additional material added to the ply to account for manufacturing tolerances and trimming.
- Staggering: The relative positioning of the tows or tapes in adjacent layers to improve structural performance.
- Coverage: The percentage of the layup surface that should be covered by the ply, typically set to 100 percent.

Funded by the European Union

- Minimum Cut Length (MCL) Extension: The minimum length of a tow or tape that can be placed, which is a limitation of the AFP process mechanics.
- To introduce defects in the simulation, the configuration generator allows users to modify certain parameters:
    - Angle Variations: Instead of specifying a single angle value, users can input a range of angles to simulate misalignment defects. For example, instead of a perfect 0-degree or 90-degree angle, a small deviation (e.g., ±0.1 or ±0.2 degrees) can be added.
    - Gap/Overlap: By specifying a positive gap value, users can simulate gaps between the tows or tapes. Conversely, by specifying a negative gap value, users can simulate overlaps where the tapes are laid on top of each other.

The remaining parameters, such as manufacturing excess, staggering, coverage, and MCL extension, are primarily dependent on the manufacturing process and can be defined by the end user based on their specific requirements.

Once the user has defined the ply using the configuration generator, they can generate a configuration file and save it to the desired location, typically in the same folder where they plan to run the simulation. This configuration file serves as an input to ADDPath®, providing the necessary information to simulate the AFP process, including any intentionally introduced defects.

3.1.3 Defects

In the AFP process, various defects can occur due to factors such as tow sliding tolerances, robotic inaccuracies, loss of tension, and the curvature of the layup surface. These defects are simulated in ADDPath® to better understand their impact on the final product quality and to generate data for the permeability surrogate model and RTM simulation.

Gap

Gaps are simulated in ADDPath® by introducing a positive spacing between the tows or tapes. This is achieved by specifying a positive value within a given range, representing the gap size. The gaps introduced in the simulation will be captured when updating the mesh for the workflow in PAM-RTM and other subsequent processes

Funded by the European Union

Overlap

Overlaps are simulated in ADDPath® by specifying a negative value for the gap between the tows or tapes. This negative value causes the tapes to overlap in the simulation, representing the overlap defect that can occur in the actual AFP process.

Misalignment

Misalignment defects are simulated in ADDPath® by introducing a slight variation in the input angle for the entire layer. Instead of specifying the perfect 0-degree or 90-degree angle, a small deviation (e.g., 0.1 or 0.2 degrees) is added to the input value. This simulates the misalignment of the layer with respect to the previous layers.

Randomization

As the defects are not currently sourced from the actual AFP process, they are randomized in the simulation to complete the workflow. Randomization is applied to the above-mentioned defects (gaps, overlaps, and misalignment) within their respective ranges. This allows for the generation of various scenarios that can be used to assess the impact of these defects on the final product quality and to provide input data for the permeability surrogate model and RTM simulation.

3.2 Strategy and trajectory planning

Once the key parameters have been defined, such as the layup surface, boundary surface, and layup configuration, the next step is to select the appropriate planning strategy based on the type of surface being processed. ADDPath® offers different planning strategies for various surface types, each with its own set of considerations and algorithms.

For the majority of the structures in this project, the default planning strategy selected is the open shape 2D and 3D strategy, as it is suitable for most of the encountered geometries. This strategy allows for efficient trajectory planning and tape placement while considering the specified defects and limitations.

Funded by the European Union

3.3 Planning strategy

Open Shape 2D and 3D

For open surfaces where no edges are touching, the open shape 2D and 3D planning strategy is employed. This strategy is suitable for both flat and curved geometries, which is the case for most structures in this project. The planning algorithm generates a central profile based on the defined 0-degree and 90-degree directions in the layup definition. From this central profile, the first curve is generated on the surface, approximately at the middle of the layup surface. The algorithm then offsets the curves, ensuring that they adhere to the specified limitations of gap, overlap, over-travel, minimum cut length, and other relevant parameters. During the planning process for the first layer, the software generates trajectories and offsets them on the 2D or 3D surface. In this strategy, the length of each placed tape is relatively short, with a defined beginning and end. The angle definition and orientation of the tapes are determined based on the specific requirements of the layup.

Closed Shape

For closed surfaces, such as pipes or tubes, where the edges are touching, a different planning strategy is employed. In these cases, the orientation and continuation of the tapes have significant implications. For example, a 90-degree path perpendicular to the rotary axis would result in a never-ending path. Therefore, the planning strategy for closed shapes takes into account the coverage of the surface and the specific limitations associated with the geometry. In closed shape planning, the strategies differ based on the desired coverage and the constraints imposed by the surface. The software takes into account the unique characteristics of closed surfaces and generates appropriate paths to ensure proper coverage and adherence to the defined parameters.

3.3.1 Ply drop-offs

Ply drop-offs refer to the plies that terminate within the layup and do not span the entire layup surface, an example of this is shown in the Figure 3.4. These ply drop-offs allow designers to selectively stiffen the structure and provide reinforcement in specific areas, offering greater flexibility in the design process. However, the definition and planning of ply drop-offs pose significant challenges from a manufacturing perspective.

Funded by the European Union

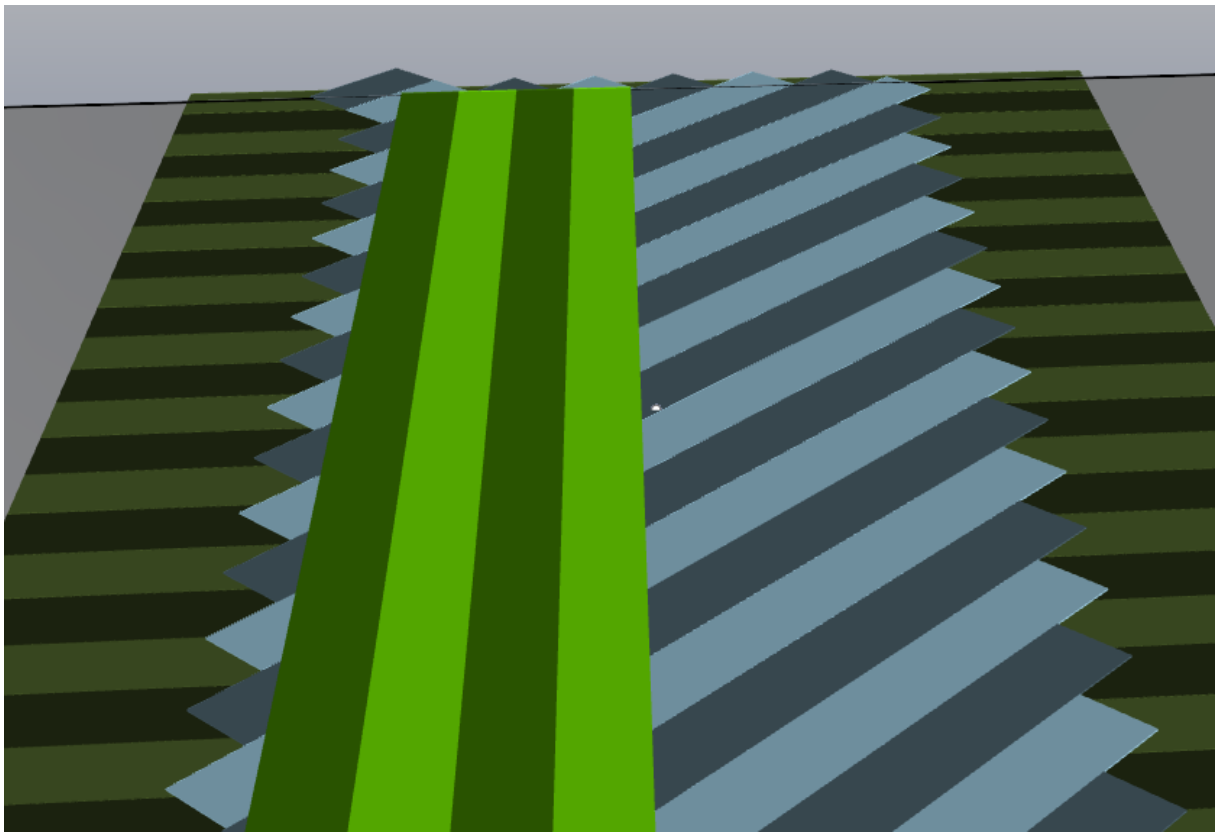

Figure 3.4 Ply drop-offs in flat plat laminate with different orientation

To address these challenges, modifications are planned for the next stage of the project to enhance the ply definition interface. The interface will be updated to incorporate the definition of ply drop-offs from specific edges of the surface. This improvement will enable users to specify the location and extent of the ply drop-offs within the layup.

In cases where ply definitions are already available from analysis software, these definitions can be used as input to define non-rectangular ply drop-offs. This integration allows for seamless transfer of ply drop-off information from the design stage to the manufacturing planning stage.

In the main use case of the Outlet Guide Vane (OGV), there are ply drop-offs present in either direction. The goal for the next phase of the project is to simulate these ply drop-offs in the OGV, incorporating the defects and using the updated ply drop-off definition options.

Funded by the European Union

3.4 Tow generation and defect identification.

3.4.1 Tape geometry generation

In the CAELESTIS workflow, the tape geometry generation is performed within ADDPath®. Unlike typical offline planning software, ADDPath® generates the exact geometry of the tape for each ply and pass. This is essential for accurately simulating defects and understanding their impact on the layup process and the final product quality.

The tape generation process in ADDPath® involves creating a cross-section of the tape along the path curve length and draping it onto the surface. This ensures that the generated tapes conform to the layup surface and avoid any floating tapes in case of ply drop-offs or ply endings. By generating the precise tape geometry, ADDPath® accounts for the specific characteristics of the surface and the presence of any ply terminations.

3.4.2 Defect identification

After the tape geometry generation, ADDPath® identifies the defects based on the defined gaps, overlaps, and misalignments. These defects are now ready to be measured and analyzed at any given point in the laminate.

For any specific point in the laminate, ADDPath® can determine the proximity and influence of certain defects. It can calculate the distance from a point to a particular defect and estimate the effect of those defects on that specific location. This readiness to measure and analyze defects is a key aspect of the defect identification stage in the CAELESTIS workflow.

3.5 Ready and output data for PAMRTM

3.5.1 Centroid data update

The centroid data, initially imported in the format of Element ID, X, Y, and Z coordinates, serves as the basis for evaluating defects at each point and generating a comprehensive defect report. The updated centroid information includes the following details for each point:

- ID: The mesh element ID obtained directly from the PAM-RTM® software.
- Coordinates: The X, Y, and Z coordinates of the centroid point.
- Ply Orientation: The orientation of the laminate at the given point, considering all the plies that will be present.

Funded by the European Union

- Normal: The normal vector of the layup surface at the particular point.
- 0° Layer Orientation: The vector defining the 0-degree orientation.
- Distance: The distance of the point from the layup surface.

In addition to these basic parameters, ADDPath® also provides information about the presence and characteristics of gap and overlap defects at each centroid point. The defect information is represented using a notation table, which includes the following columns:

- Gap: Indicates the presence of a gap defect (0 for no gap, 1 for gap).
- Distance To Gap: The distance from the centroid point to the nearest gap defect (9999 if not in any feature and further than 2.5mm from any gap).
- Size of Gap: The size of the gap defect, if present.
- Overlap: Indicates the presence of an overlap defect (0 for no overlap, 1 for overlap).
- Distance To Overlap: The distance from the centroid point to the nearest overlap defect (9999 if not in any feature and further than 2.5mm from any overlap).
- Overlap Size: The size of the overlap defect, if present.

3.5.2 Terminology

The notation below provides a clear interpretation of the defect presence and proximity at each centroid point. The terminology used in the table is as follows:

- A value of 0 in the "Feature Present" column indicates the absence of the defect.
- A value of 1 in the "Feature Present" column indicates the presence of the defect.
- A value of 9999 in the "Distance to Feature" column indicates that the point is not in any feature and is further than 2.5mm from any defect.
- A value of 0 in the "Distance to Feature" column indicates that the point is inside an overlap or very close to it.
- A value of 1.15 in the "Distance to Feature" column indicates that the point is less than 2.5mm away from an overlap.
- A value of 2.34 in the "Distance to Feature" column indicates that the point is less than 2.5mm away from a gap.

Funded by the European Union

4 PERMEABILITY SURROGATE GENERATION (ITA)

Permeability is a fundamental property that describes the ease with which a fluid can move through a porous medium, such as composite materials. This property plays a crucial role in various manufacturing processes, particularly in the production of advanced composite components through Automated Fiber Placement (AFP) and Resin Transfer Molding (RTM).

In the aviation industry, accurate prediction and control of permeability are essential for ensuring the quality and performance of composite structures. Proper permeability is critical to achieving uniform resin distribution during manufacturing processes like AFP-assisted RTM. Optimal permeability ensures that the resin infiltrates the fiber preform uniformly, leading to a composite material with consistent mechanical properties and structural integrity.

The permeability of AFP materials presents unique challenges compared to traditional woven composite materials due to the preferential channels that appear between tows to avoid overlap defects. Therefore, there is a need to develop specialized surrogate models that can accurately predict permeability in AFP materials, taking into account the intricacies of their manufacturing processes.

Additionally, the significant advantage provided by AFP, the automation of preforms generation, can also be a source of potential defects such as misalignments, gaps, or overlaps that unavoidably affect the local permeability of the preform.
Thus, an innovative model has been developed to specifically predict permeability in AFP materials. This model leverages integrated simulations of AFP and RTM processes to capture the complex interplay between material properties, manufacturing parameters, and permeability.

Figure 4.1 shows the workflow developed to generate the permeability Reduced Order Models (ROMs). The entire workflow is developed in Python scripts and then included in a PyCOMPSs

Funded by the European Union

workflow in WP2 to reduce and optimize the computational time. We can identify four main steps:

1. Data generation and model training.
2. Preprocess for the CFD simulations.
3. CFD simulation.
4. Postprocess of the simulations.

Data generation and model training are responsible for generating the cases to be used for each of the training sessions and for generating the ROM data.

Once a battery of cases to be executed has been selected, we move on to the preprocessing part of each case. At this stage, the RVE geometry is generated using an in-house Python script connected to the labeling of the interior volumes and the generation of the mesh. Once the mesh is labelled, the three simulations necessary to calculate the permeability tensor are set up.

The third step involves the execution of the three CFD simulations, with flows in X, Y, and Z directions. The software used for these simulations is Alya, BSC's own software for optimal parallelization in HPC.

Finally, the velocity and pressure results of the three simulations and fiber volume fraction (FVF) for each of the interior volumes are post-processed together, permeabilities are calculated, and labels are assigned to each interior volume. The results of all simulations are merged and taken to ROM training in Twinkle, ITA's own software using Canonical Polyadic Decomposition (CPD).

Funded by the European Union

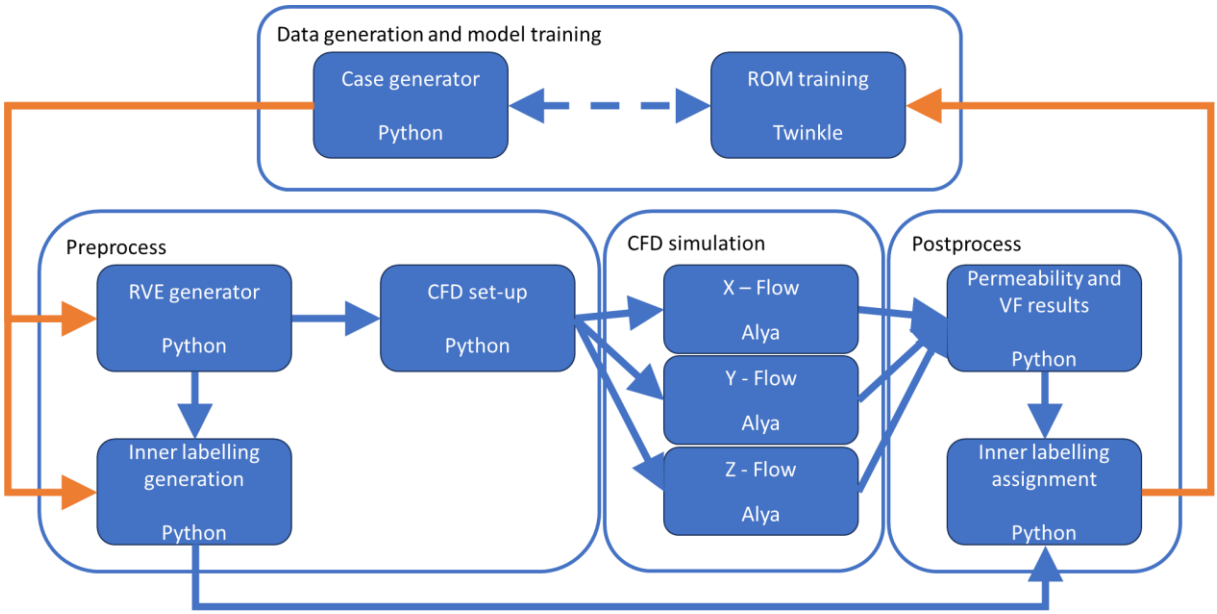

Figure 4.1: Workflow developed to generate permeability ROM.

The calculation of permeabilities to feed simulation models of the RTM process through meso-scale CFD simulations is a widespread practice. However, these models are usually in the order of 1 to 5 mm because for traditional woven fabrics this is sufficient. However, tows can be up to more than 25 mm wide in case of AFP-assisted RTM processes, which increases the complexity of meso-scale models. In addition, the surrogate permeability model connecting AFP and RTM simulations must take into account defects in the placement of the tows, which are usually in the order of a few millimeters. Furthermore, in order to make optimal use of these models, the meshing strategy and element size at the next scale (RTM) must be taken into account in the permeability model. For all these reasons, we decided to generate meso-scale RVEs models from which interior volumes are obtained and labelled according to their geometric characteristics, similar to the way elements are generated in the RTM simulation. Figure 4.2 shows an RVE with an overlap and highlights an inner volume as a demonstrator.

Funded by the European Union

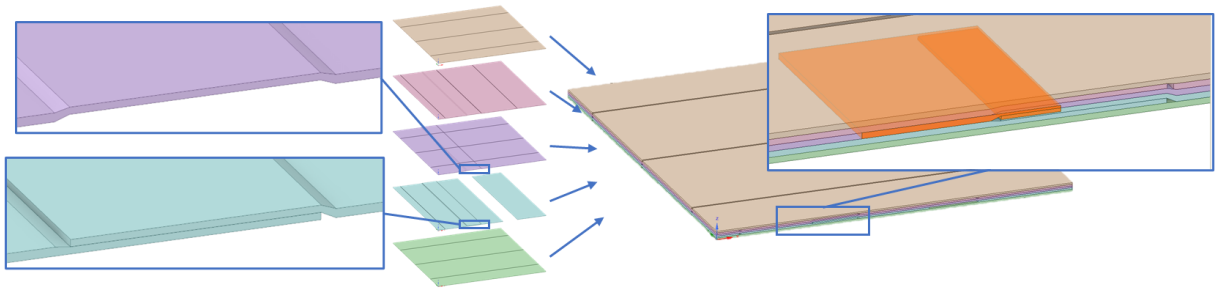

Figure 4.2: Example of an RVE consisting of 5 layers arranged as 0/90/0/90/0 with overlap defect. An inner volume is highlighted as a demonstrator.

Through the development and application of this surrogate model, the objective is to advance the understanding and prediction of permeability in AFP materials, contributing to the optimization of manufacturing processes and the design of high-performance composite components for the aviation industry.

4.1 RVE generation

The RVE generator creates the geometry and mesh necessary to calculate the permeability tensor. RVE generator gets the information of each case from the case generator and uses that information to develop a geometry and mesh with the required features. Figure 4.1 shows the connection of this module within the permeability workflow, where the case generator provides information related to:

- Tows and gaps geometry.
- Defects characteristics.
- Mesh attributes.

Using the RVE generator not only has the possibility of automating the geometry generation without taking part in the process, but also the mesh of the CFD model. In addition, meshes coming from REV generator are prepared to apply periodicity conditions in CFD simulations.

TexGen

For geometry generation, there are specific tools such as TexGen for RVE in composite materials. TexGen is an open-source software for modelling the geometry of textile structures.

Funded by the European Union

TexGen is used for a variety of properties, including textile mechanics, permeability, and composite mechanical behavior.

Figure 4.3 Traditional woven fabric generated using TexGen[1].

Using the user interface is possible to generate wovens, Figure 4.3 shows a traditional woven fabric generated using TexGen, but it is not possible to represent the defects that appear during the AFP process. To solve that, a specific TexGen-Python script has been created, importing TexGen's own libraries allows to represent the tows in the desired way using its capabilities. Figure 4.4 shows the representation of one case generated using the specific TexGen-Python script.

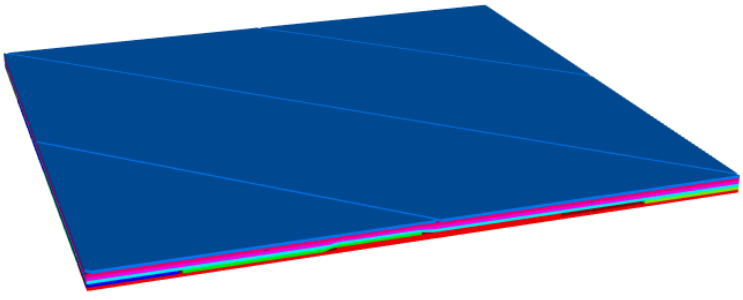

Figure 4.4 Geometry generated using in-house python script + TexGen's libraries.

[1] https://texgen.sourceforge.io/index.php/Main_Page

Funded by the European Union

TexGen has its own meshing techniques to generate the voxel mesh required for the CFD simulations. TexGen requires information about the number of voxels in each direction, X, Y and Z. With the geometry generated (including domain dimensions) and the required information, TexGen divides each side of the domain in the number of voxels required. With that information it builds the complete voxel mesh. For providing the attributes to each voxel, TexGen checks the centroid of the voxel, and tow or resin properties are assigned depending on its location.

Tows are generated using nodes located in the domain. Nodes belonging to the same tow are joined by a path and then, a surface is extruded through the path. Figure 4.5 shows an example of how the tows are created.

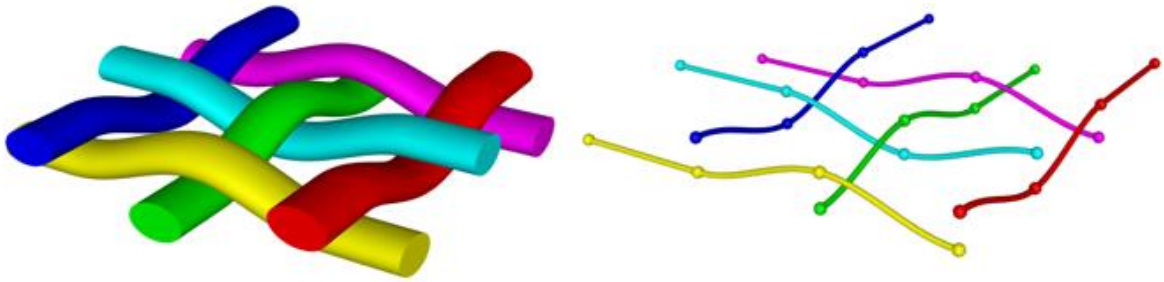

Figure 4.5 Woven textile and its nodes and paths.

Once the mesh is generated, TexGen exports three files: inp, ori and eld. The inp file contains the information of the mesh. The ori file has the orientation vector of each element. For calculating this information, TexGen uses the paths showed in Figure 4.5. The .eld file contains information about volume fraction, distance of element from the surface of the yarn and location. These three files provide the information required for setting up the CFD simulations.

Funded by the European Union

Once the mesh is generated in the Abaqus format (inp, ori, and eld), a custom Python script is employed to convert these files to the Alya format while simultaneously setting the boundary conditions. This ensures that the model is fully prepared for the subsequent CFD simulations.

However, as mentioned above, TexGen is oriented to the generation of traditional woven textiles, and some problems have been found trying to represent AFP defects. The difference between defects and tows dimensions makes TexGen not the best option as a tool for the RVE generation. As Figure 4.6 shows, the resolution of TexGen is not enough to consider the defects that appear in the AFP process.

Figure 4.6 TexGen representation of AFP defects and a mesh generated.

In-house Python script

Due to TexGen resolution problem, an in-house Python script has been developed to generate the geometry and the mesh of each case. Similar to TexGen, the script obtains input values from the case generator to finally create a mesh in Alya format. With the information obtained, the in-house Python script creates the surfaces of the tows. This works considering sections of tows. For tows without defects, it generates two sections, one at the beginning and the other at the end, and the script creates a rectangular section. For tows where the defect has an influence, there can be two sections or more depending on the orientation of the tow, and the sections are not rectangular, they are created by points. Figure 4.7 and Figure 4.8 show the two different ways of generating tows.

Once the geometry is created, the mesh must be built. There are different approaches for the discretization of the mesh, such as modifying the number of elements per layer, number of elements per gap or the size of each element.

Depending on the discretization parameters, the in-house Python script calculates the total number of elements. With this information, the RVE is divided into the elements required, and

Funded by
the European Union

after that, the script checks if the elements are into a tow or in the resin zone. For calculating the orientation, the procedure is similar as TexGen does.

Therefore, our in-house Python script streamlines the entire process: it generates the mesh, retrieves the properties of each element, calculates its orientations if it belongs to a tow, and finally produces the mesh files and Alya boundary conditions. This optimization allows us to bypass TexGen and create the final files directly in a single step, enhancing the efficiency of the RVE model creation process.

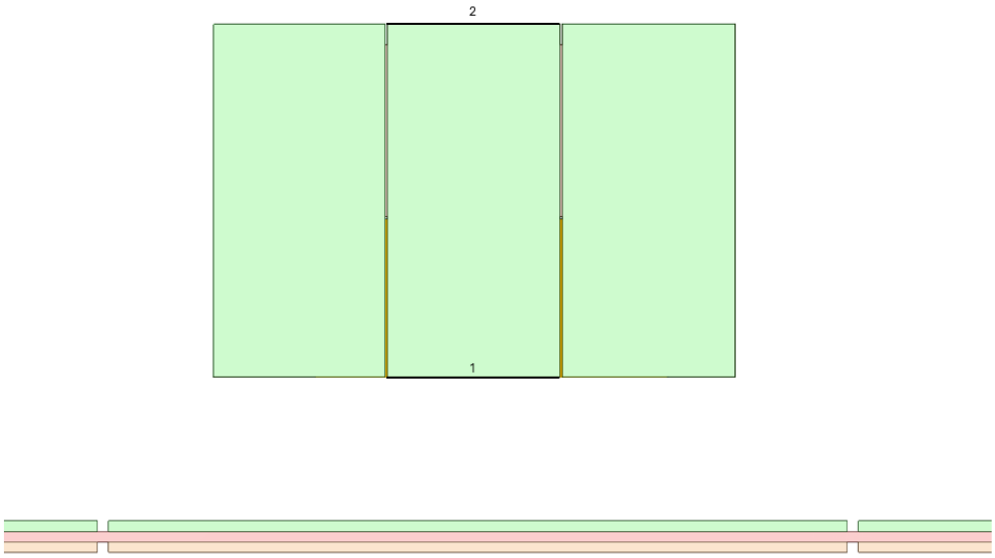

Figure 4.7 Tow with no defects generated by rectangular section.

Funded by
the European Union

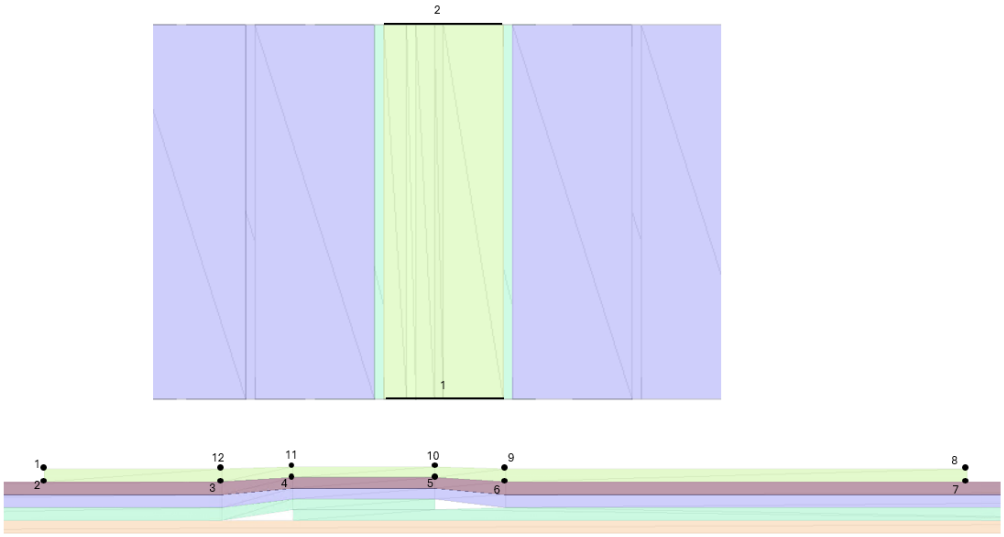

Figure 4.8 Tow with defect generated by section points.

Figure 4.9 shows a mesh generated using the In-house Python script. As it is possible to see, the In-house Python script mesh is more accurate that the one showed in Figure 4.6. This happens because the In-house Python script generates more precise geometry, so when it checks if the elements belong to a tow or to the resin, there are note errors assigning element properties.

Figure 4.9 Mesh generated by the In-house Python script.

Geometry details

Regarding tow geometry, case generator provides information about the width, height and programmed gap between tows. Also, the number of tows required in the RVE is obtained, using this to calculate the dimension of the RVE and thus the length of the tows. Figure 4.10 shows the geometry parameters in generated tows.

Funded by the European Union

Figure 4.10 Tow geometry provided by the case generator.

To ensure proper application of periodicity in the CFD model, tows are positioned such that gaps never occur at the end of the RVE.

Another important information is the orientation of each tow and the number of layers (tows belonging to the same layer have the same orientation). This information is also provided by the case generator, and with this the required geometry information for a case without defects is complete.

As mentioned above, the in-house Python script is intended to represent the defects that occur during the AFP process. The most common defects are the separation of tows more than programmed, generating a gap between them, and the placement of one tow on top of another generating an overlap. Figure 4.11 shows an overlap and a gap generated by the in-house Python script.

Figure 4.11 Overlap (top) and Gap (bottom) generated by the In-house Python script. Orange tow is the wrongly positioned.

For representing the defects, information about them is required. The main considerations of defects are:

- Defects will not be corrected, which means that an overlap will result in a gap, and vice versa.

Funded by the European Union

- Where there is an overlap, there are more layers than expected, and this result in lower thickness of the layer (assuming constant mold thickness).

Thus, the information necessary to define a defect consists of, type of defect, length of the defect, transition zone (left and right) from the defect to the others tows and the change of the height in the affected zone.

Once the defect is known (gap or overlap) its geometry values are required. The length of defect is used to calculate how much part of the next tow is overlaid. For the overlap this occurs because the AFP fails, and it places one tow without considering the programmed gap or even allocating it on top of the one already placed. Due to it, a gap is generated to the right of the misplaced one.

For the gap defect, the effect is similar, but the cause is the opposite. The AFP process leaves a gap (more than the programmed one) between tows, so the consequence is that the placement of the next one (which is well placed) occurs on top of the one that has been displaced. Figure 4.12 and Figure 4.13 represent the defects.

Figure 4.12 A represents the overlayed tow and B the gap generated because of the misplaced tow (overlap situation). Orange is the first tows allocated and green the second.

Figure 4.13 A represents the gap left by the AFP and B the consequence (gap situation). Orange is the first tow allocated and green the second.

Other geometry values provided by the case generator are the values of the transition zone, right and left of the overlaid area. These two values represent the length at which the upper tows are placed in their correct position. Figure 4.14 shows the representation of these transition values. For overlap and for gap defect the procedure is the same.

Funded by the European Union

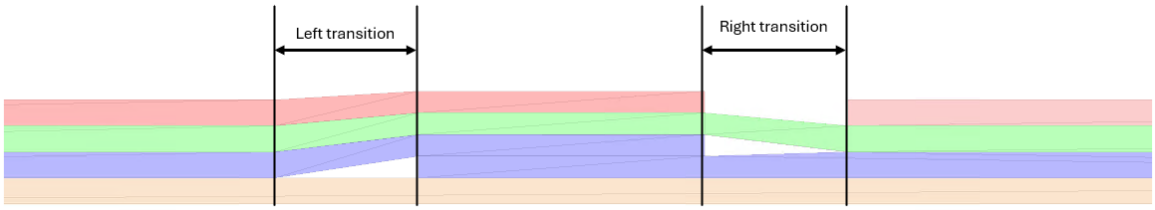

Figure 4.14 Representation of the transition zones. Tows belonging to the same layer have the same color.

Finally, the last parameter defining defects obtained from the case generator is the change of height in the affected zone. When a defect occurs, there is a zone with an extra tow through thickness due to the overlay (see Figure 4.15). So that, a parameter for reducing the height of the tows in the affected area is necessary. This is also necessary because a defect not only affect the layer in which it occurs, but it also affects the other layers.

Figure 4.15 shows this effect. The normal allocation of the tows is represented by the apostrophe layers, where six layers are placed. In the affected area, as it is possible to see, seven tows are allocated where it should be six. Layers one and seven do not modify their height, but the rest do.

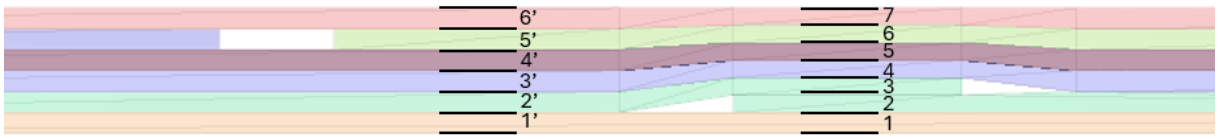

Figure 4.15 Representation of the stacking of the tows with a defect. Tows belonging to the same layer have the same color.

4.2 Case configuration

Once the mesh is available, the next step is to set up the three required cases for each single RVE geometry to obtain the permeability. A monophasic, incompressible, viscous flow through a medium containing both porous (tows) and no porous zones is simulated. The model is assumed to be fully filled of resin that flows guided by a pressure gradient imposed in a given direction (X, Y or Z, depending on the case). Therefore, the conservation of mass (continuity

Funded by the European Union

equation) for monophasic incompressible flow (Equation 1) and conservation of momentum (Equation 2) are solved:

$$(\nabla \vec{v}) = 0$$

Equation 1: Continuity equation.

$$\rho \frac{\partial \vec{v}}{\partial t} + \nabla \cdot (\rho \vec{v}\vec{v}) = \nabla p + \nabla \cdot \left[\mu \left(\nabla \vec{v} + \nabla \vec{v}^{T} - \frac{2}{3} \nabla \vec{v} I \right) \right] + \rho \vec{g} - S_{porous}$$

Equation 2: Momentum equation.

where $\vec{v}$ is the velocity vector, ρ is the resin density, t is time, p is pressure, μ is resin dynamic viscosity, $\vec{g}$ is the gravity vector, I is the identity matrix and S_{porous} is the source term added to account for porous media,

$$S_{porous} = \left(\mu \vec{\vec{D}} \right) \vec{v}$$

Equation 3: Porous source term equation.

where $\vec{\vec{D}}$ is the inverse of the permeability tensor; $D_{ij} = \frac{1}{K_{ij}}$ with K_{ij} as the permeability components.

The resin is assumed to be an incompressible, viscous Generalized Newtonian Fluid (GNF), and density and viscosity remain constant throughout the simulation.

The physical equation described above are discretized using Finite Element Method (FEM) and stabilized using the Algebraic Subgrid Scale method[2]. The pressure Schur complement is solved using the Orthomin(1) method at each non-linear iteration and converges to the monolithic solution[3]. Momentum equation is solved with the GMRES method and the continuity equation with the Deflated Conjugate Gradient.

[2] Houzeaux, G., & Principe, J. (2008). A variational subgrid scale model for transient incompressible flows. International Journal of Computational Fluid Dynamics, 22(3), 135-152. https://doi.org/10.1080/10618560701816387

[3] Houzeaux, G., Aubry, R., & Vázquez, M. (2011). Extension of fractional step techniques for incompressible flows: The preconditioned Orthomin (1) for the pressure Schur complement. Computers & Fluids, 44(1), 297-313. https://doi.org/10.1016/j.compfluid.2011.01.017

Funded by the European Union

Regarding Boundary Conditions (BCs), external faces normal to the X-vector and external faces normal to the Y-vector are considered periodic. It is assumed that the tows are deposited on the plane normal to the Z-vector, as shown in Figure 4.16. Meanwhile, external faces normal to the Z-vector may have two possible BCs; periodic conditions for the general-purpose cases, or wall conditions (zero velocity) when studying the effect of the external walls of the mold on permeability.

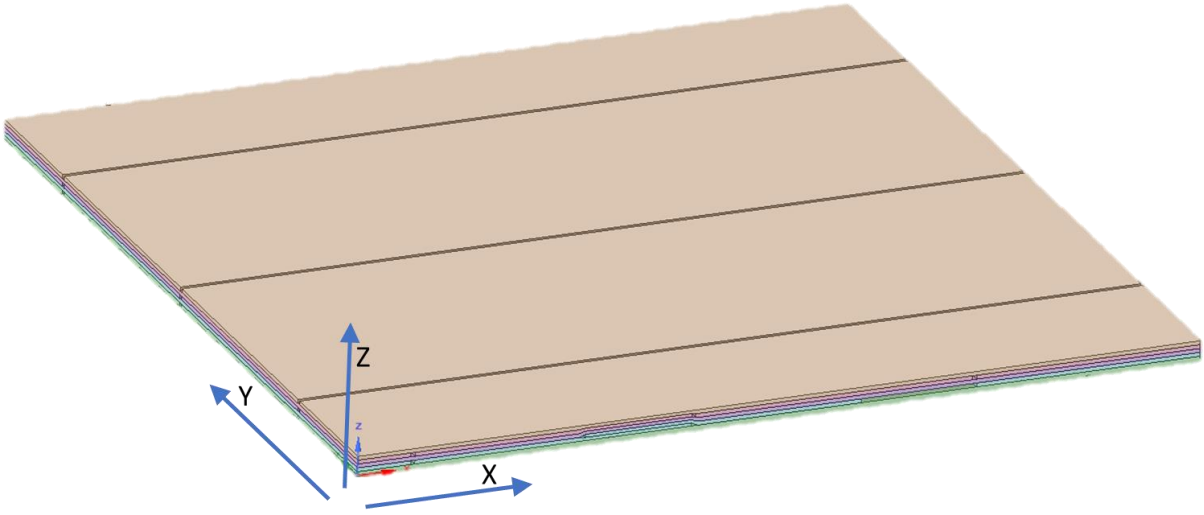

Figure 4.16: RVE geometry.

For calculating the permeability, three simulations applying pressure drops in different directions of the RVE are required (see section 4.3). The pressure gradient is imposed as a force term in the momentum equation, entering as a gravity term. Thus, pressure drop is calculated as:

$$\Delta p = \rho \vec{g} L_{dom}$$

Equation 4: Pressure drop to gravity relation.

where L_{dom} is the length of the RVE in the flow direction.

The porous source term of the elements not belonging to a tow are assumed to be zero ($S_{porous} = 0$), while for the elements belonging to a tow, it is calculated depending on the assigned permeability.

Funded by the European Union

Tows are made up of hundreds of carbon fibers aligned in one direction. Fibers have a diameter of approximately 5 µm, and the compaction depends on several manufacturing and AFP process factors.

CFD micro-scale simulations can be conducted to obtain a homogeneous representative value of permeability at this scale. However, there also exists a well-known equation describing the micro-scale permeability inside tows, known as Gebart's equation[4].

Gebart's equation is typically used to compare the results of micro-scale permeability simulations, and the value of this equation differences the longitudinal direction of the fibers and the transversal direction of the fibers:

$$K_{lon} = \frac{8 \cdot R^2 \cdot (1 - FVF)^3}{c \cdot FVF^2}$$

Equation 5: Gebart's equation for intra-tow permeability in longitudinal direction.

$$K_{per} = C_1 \cdot R^2 \cdot \left(\sqrt{\frac{FVF_{max}}{FVF} - 1} \right)^{\frac{5}{2}}$$

Equation 6: Gebart's equation for intr-tow permeability in transversal direction.

where R is the fiber radius, FVF is the intra-tow fiber volume fraction, FVF_{max} is the theoretical maximum fiber volume fraction, and c and C_1 are constant parameters.

The values of FVF_{max}, c, and C_1 depend on the selected packing arrangement, which can be either quadrilateral or hexagonal (see Figure 4.17). For the CAELESTIS project, hexagonal fiber arrangement is selected, thus the constants take the following values: $FVF_{max} = \frac{\pi}{2\sqrt{3}}$, $c = 53$, and $C_1 = \frac{16}{9\pi\sqrt{2}}$ (see Figure 4.17).

[4] Gebart, B. R. (1992). Permeability of unidirectional reinforcements for RTM. Journal of composite materials, 26(8), 1100-1133.. https://doi.org/10.1177/002199839202600802

Funded by the European Union

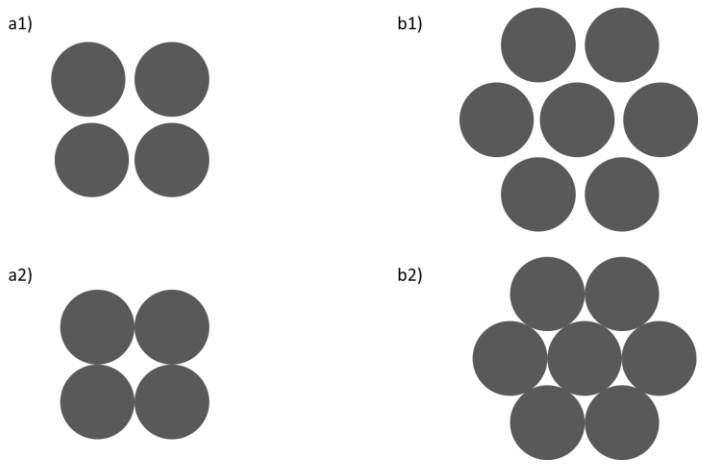

Figure 4.17: Different packing arrangements: a1) quadrilateral packing for a given FVF, a2) quadrilateral arrangement for maximum FVF, b1) hexagonal arrangement for a given FVF, and b2) hexagonal arrangement for maximum FVF.

Macro-scale fiber volume fraction of the FOGV is a design parameter that can be modified depending on the performance and manufacturing requirements and is modified by the number of tows introduced in the mold (number of stacked tows and distance between contiguous tows). Therefore, assuming the width of the tow and distance between tows as constants, intra-tow FVF (FVF^{micro}) can be obtained as:

$$FVF^{micro} = \frac{FVF^{macro}(w+g)}{2}$$

Equation 7: Micro-macro FVF assumption.

where w is the tow width, and g is the programmed distance between tows. Thus, the intra-tow FVF will depend on the macro FVF, and following the Gebart's equation for hexagonal fiber arrangement, intra-tow permeability will be in the order of 5e-13 m2 to 4e-15 m2 depending on the FVF and longitudinal or transversal direction (see Figure 4.18).

Funded by the European Union

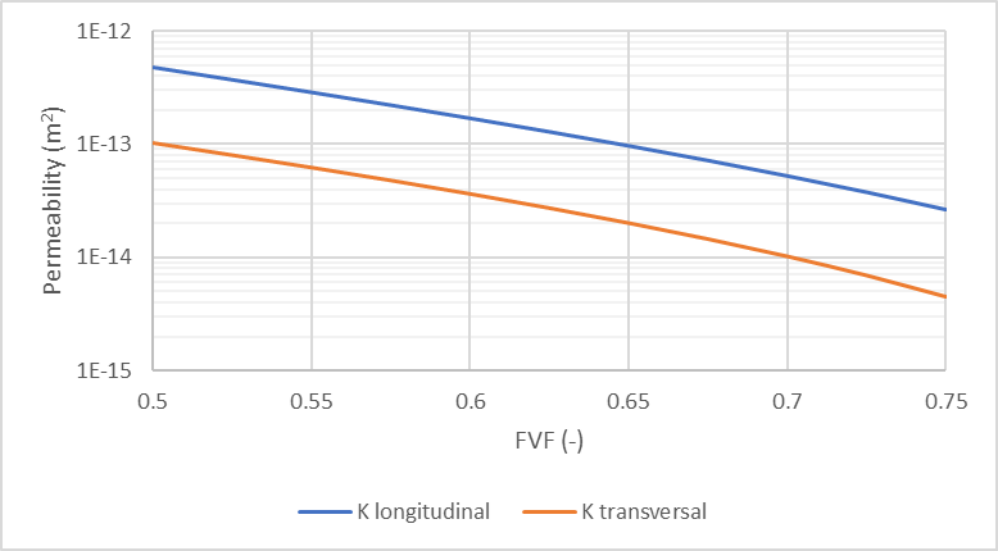

Figure 4.18: Gebart's permeability depending on the fiber volume fraction.

Thus, local permeability tensor of each element is calculated depending on the FVF of that element with the Gebart's equation with hexagonal packing:

$$K^{local} = \begin{pmatrix} K_{long} & 0 & 0 \\ 0 & K_{trans} & 0 \\ 0 & 0 & K_{trans} \end{pmatrix}$$

Equation 8 Local permeability tensor

and then transforming from local to global coordinates depending on the orientation generated in the RVE generator:

$$K^{global} = A \cdot K^{local} \cdot A^T$$

Equation 9 Local to global permeability transformation

where A is the transformation matrix.

4.3 Postprocessing

Two main results are required from the CFD simulations: permeability tensor, and fiber volume fraction.

To obtain the permeability tensor we need to postprocess the velocity and pressure gradients from the three simulations at the same time:

Funded by the European Union

$$\begin{bmatrix} K_{xx} \\ K_{xy} \\ K_{xz} \\ K_{yx} \\ K_{yy} \\ K_{yz} \\ K_{zx} \\ K_{zy} \\ K_{zz} \end{bmatrix} = \mu \begin{bmatrix} \nabla P_x^1 & \nabla P_y^1 & \nabla P_z^1 & 0 & 0 & 0 & 0 & 0 & 0 \\ 0 & 0 & 0 & \nabla P_x^1 & \nabla P_y^1 & \nabla P_z^1 & 0 & 0 & 0 \\ 0 & 0 & 0 & 0 & 0 & 0 & \nabla P_x^1 & \nabla P_y^1 & \nabla P_z^1 \\ \nabla P_x^2 & \nabla P_y^2 & \nabla P_z^2 & 0 & 0 & 0 & 0 & 0 & 0 \\ 0 & 0 & 0 & \nabla P_x^2 & \nabla P_y^2 & \nabla P_z^2 & 0 & 0 & 0 \\ 0 & 0 & 0 & 0 & 0 & 0 & \nabla P_x^2 & \nabla P_y^2 & \nabla P_z^2 \\ \nabla P_x^3 & \nabla P_y^3 & \nabla P_z^3 & 0 & 0 & 0 & 0 & 0 & 0 \\ 0 & 0 & 0 & \nabla P_x^3 & \nabla P_y^3 & \nabla P_z^3 & 0 & 0 & 0 \\ 0 & 0 & 0 & 0 & 0 & 0 & \nabla P_x^3 & \nabla P_y^3 & \nabla P_z^3 \end{bmatrix}^{-1} \cdot \begin{bmatrix} V_x^1 \\ V_y^1 \\ V_z^1 \\ V_x^2 \\ V_y^2 \\ V_z^2 \\ V_x^3 \\ V_y^3 \\ V_z^3 \end{bmatrix}$$

Equation 10: Permeability calculation.

where K is the permeability tensor, P is the pressure gradient, V is the average fluid velocity, subscripts x, y, and z describe the directions, and 1, 2, and 3 describe the numerical simulation performed in each direction.

Then, we have to solve a linear system of 9 equations and 9 unknowns. Nevertheless, due to the convergency precision of the CFD simulations, resultant permeability tensor could be unsymmetrical. We force the symmetry of the permeability tensor combining Equation 10 and Equation 11, thus leading to 9 equations and 6 unknown over-determined system (Equation 12).

$$\begin{cases} K_{xy} = K_{yx} \\ K_{xz} = K_{zx} \\ K_{zy} = K_{yz} \end{cases}$$

Equation 11: Symmetry assumption.

$$\begin{bmatrix} K_{xx} \\ K_{xy} \\ K_{xz} \\ K_{yy} \\ K_{yz} \\ K_{zz} \end{bmatrix} = \mu \begin{bmatrix} \nabla P_x^1 & \nabla P_y^1 & \nabla P_z^1 & 0 & 0 & 0 \\ 0 & \nabla P_x^1 & 0 & \nabla P_y^1 & \nabla P_z^1 & 0 \\ 0 & 0 & \nabla P_x^1 & 0 & \nabla P_y^1 & \nabla P_z^1 \\ \nabla P_x^2 & \nabla P_y^2 & \nabla P_z^2 & 0 & 0 & 0 \\ 0 & \nabla P_x^2 & 0 & \nabla P_y^2 & \nabla P_z^2 & 0 \\ 0 & 0 & \nabla P_x^2 & 0 & \nabla P_y^2 & \nabla P_z^2 \\ \nabla P_x^3 & \nabla P_y^3 & \nabla P_z^3 & 0 & 0 & 0 \\ 0 & \nabla P_x^3 & 0 & \nabla P_y^3 & \nabla P_z^3 & 0 \\ 0 & 0 & \nabla P_x^3 & 0 & \nabla P_y^3 & \nabla P_z^3 \end{bmatrix}^{-1} \begin{bmatrix} V_x^1 \\ V_y^1 \\ V_z^1 \\ V_x^2 \\ V_y^2 \\ V_z^2 \\ V_x^3 \\ V_y^3 \\ V_z^3 \end{bmatrix}$$

Equation 12: Permeability calculation forcing symmetry.

Funded by the European Union

The overdetermined system is solved to the last square sense, and eigenvalues (λ_i) and eigenvectors ($\boldsymbol{w}_i$) are computed, which constitute principal values and direction of the permeability:

$$\overline{\overline{K}} \times \boldsymbol{w}_i = \lambda_i \boldsymbol{w}_i$$

Equation 13 Eigenvalues and eigenvectors.

Figure 4.19 shows an example of the velocity results in the x-flow direction for a specific RVE with overlap.

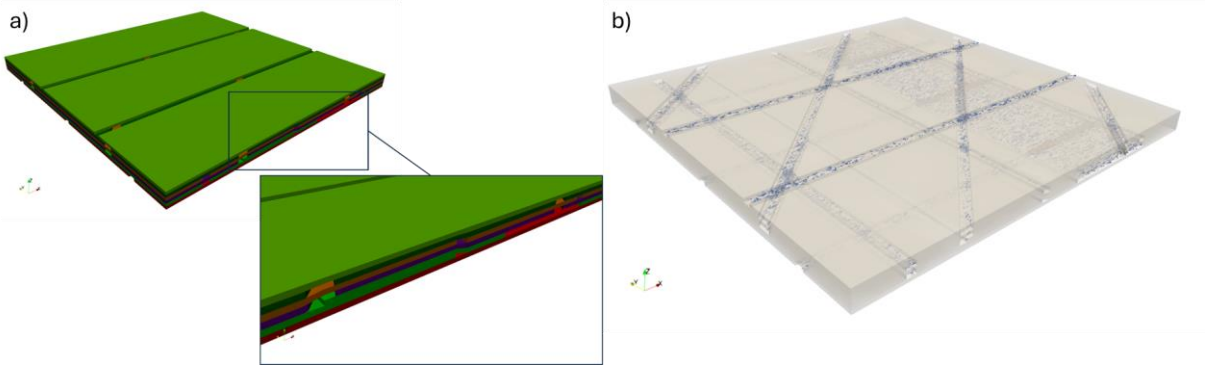

Figure 4.19 CFD simulation: a) geometry of an RVE with overlap, and b) velocity arrows from CFD results.

Labelling

In order to develop a model capable of real-time operation, we need to simplify the problem without disregarding important information. We opted for aggregating elements and classifying these sets of elements based on their contents. Since the fiber matrix follows very strict patterns, even when accounting for defects, and permeability of a region should not be dependent on surrounding geometry, we can stablish a correlation between the positions of these sets relative to defects or programmed gaps and their resulting permeability.

To train the surrogate models, we need to label the sets of our own RVEs, which we can do since both the rules for placing tows as well as defects are known to us. Using this information in conjunction with the position of the sets, we can determine their relative positioning concerning defects, the layer in which they are, and the orientation of the fibers.

To accomplish this, we go through the sets and compare their position to the position of the programmed gaps, assuming no defects, and label the sets if they fall within half the length of a set plus half the length of a programmed gap within its layer. Then, if there is a defect on

Funded by the European Union

the simulation, we check if the set is within the defect area of influence, similarly as we did earlier with programmed gaps, and then label the set accordingly.

Furthermore, we can then aggregate the sets to be flexible to different size of surrogate elements at no higher cost in simulations. To achieve this, we consider all the preexisting labels in a set and the sets that surround it within the same layer and take the maximum value for the defect flags (-1 is no defect, 0 is defect within the layer and 1 through 6 are an overlap *n* layers below). Consequently, if a set contains a defect, the aggregate will also contain it. The size of the set is computed depending on how many sets we aggregate, and the defect size is equal to the defect size of the set with a higher flag as previously mentioned. The rest of the values should be equal in all the sets since the orientation depends on the layer, and all belong to the same layer, so we just average them.

Lastly, it should be noted that this approach allows us to extract a substantial amount of data from an RVE. Specifically, the extracted data is proportional to the ratio of our domain's length to the set's length, squared, multiplied by the number of layers. Even when aggregating sets, the resulting aggregates overlap, yielding diverse data from the same elements of the mesh.

4.4 Surrogate training

As previously discussed, the permeability of a set should not be influenced by anything other than its geometry and the orientation of the layers that it includes. Furthermore, its geometry is only dependent on the orientation and the defects it contains.

Hence, we decided to label the sets in relation to the defects that are present within it and the orientation of the tows in its layer and the contiguous ones. This is relevant in case there is an overlap, or if it is the bottom-most or top-most layer. Present defects are any overlap happening over, below or inside the set, and gaps, being programmed or not, whose effects are noticeable when looking only at the elements present in the set. This results in essentially five different cases that represent any possible occurrence.

Funded by the European Union

Firstly, there are the element sets that happen purely inside a tow, where orientation and intra-tow FVF should be the only variables affecting. Secondly, the sets that contain only a gap and any amount of tow, but no overlap. In these cases, knowing the size of the gap and the size of the element should be enough to stablish a dependency with the permeability. Thirdly, there is the overlap case, where in this case and the following ones we do need a way to model their impact. Fortunately, to determine the permeability we only need information of the set's geometry, and the geometry of the set is easily described only from the distance to the center and the size of the overlap. Hence that is the only input needed to calculate the permeability. Some examples of these cases are illustrated in Figure 4.20.

Figure 4.20 Example of areas of influence of an overlap (red) and gaps (green) some possible sets are highlighted in maroon, from left to right there would be two sets that belong to the overlap case, a set that has no defect and two sets that belong to the gap case.

However, the relation between the geometry and permeability is less straightforward than the gap case, and here is where the surrogate training becomes very useful. Within this last case we may want to separate the case where the overlap happens in the same layer or in subsequent ones. In case the overlap happens in subsequent layers, we will need the layer distance as an input variable to the surrogate model. Lastly there is the case of having an overlap in a different layer and a gap in the same layer, which, similarly to the previous case, can be easily described by the distance and size of the gap and overlap but its permeability is not easily deduced, and these are the cases were a surrogate model will be of great importance.

As mentioned in the previous paragraph, we are training the surrogate model using sets of elements defined by their position relative to defects and fiber orientation. This is because these factors are sufficient to describe the geometry of a set accurately. This results in the need for training five models as opposed to one, however, the difficulty of training these models is reduced in terms of required simulations, and their explainability is enhanced, since the cases are similar to other occurrences of the same case, and it can be checked if the relation between permeability with the distance and size of the defects follows a logical trend.

Funded by the European Union

The inputs that we will use in the surrogate training are:

- Orientation of in-set and contiguous layers.
- Length of the set.
- Defect occurrence, whether it is a gap, overlap, both, or none, and in the overlap's case how many layers of distance are between the set and the overlap.
- Distance to gap or overlap in case it is visible inside the set.
- Size of gap or overlap that is visible inside the set.

Finally, the outputs will be the principal components and directions of the permeability tensor, and FVF of the element. Furthermore, the positional information of the sets will also be considered in order to restore the permeability mesh after evaluating.

The surrogate model is an algorithm based on Tensor Rank Decomposition (TRD) that approximates the response surfaces of multi-dimensional data as a sum of products of one-dimensional functions. This data is collected from the cases proposed in the precious sections,

$$F(v_1, \dots v_D) = \sum_{t=1}^{T} \alpha_t \prod_{d=1}^{D} f_{t,d}(v_d)$$

Equation 14 Tensor Rank Decomposition.

where D is the number of dimensions, T is the degree of approximation of the ROM, α_t is the weighting coefficients, and $f_{t,d}$ the one-dimensional functions (one for each input variable).

The use of this model allows for separating each variable's contribution to the system's output, enabling interpretable results. As shown in Figure 4.21. we can see the contribution of the different variables to a given output, generally the first order has a much bigger alpha and represents the main contribution with the second and consecutive orders being corrections.

Funded by the European Union

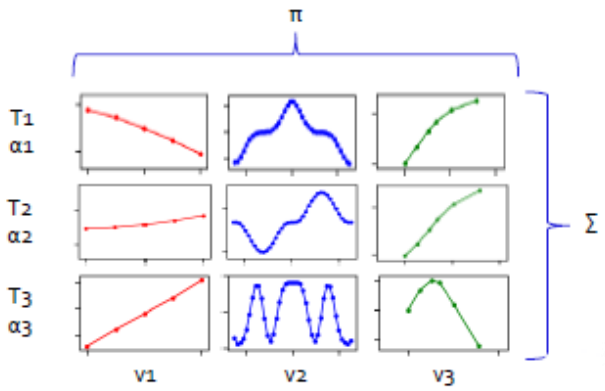

Figure 4.21 Representation of the contribution of 3 variables approximated to the 3rd order.

4.5 AFP-RTM connection and permeability surrogate assessment

As previously explained in section AFP Digital Twin in the global workflow, the main function of the surrogate permeability model is to bridge the AFP simulations (AddPath) with the RTM simulations (PAM-RTM) within the overall simulation workflow. Therefore, the importance of defining the surrogate model considering these simulations and their particularities.

Additionally, the model should be evaluated without supervision, thus the inputs need to be meticulously defined to prevent any errors during the workflow execution.

To address this, the variables shown in Table 2 have been defined, which unequivocally identify each element of the model and enable its connection to the permeability model. These variables are:

- Layer number: denotes the layer to which it belong.
- Ply orientation: indicates the orientation of the layer to which it belongs.
- Normal: the normal direction of the deposition surface.
- 0º layer orientation: represents the orientation vector defining the 0-degree orientation of the layer.
- Distance: indicated the distance from the deposition surface to the element centroid.
- Gap: flags whether the element contains a gap.
- Gap distance: measures the distance from the element to the gap.
- Gap size: quantifies the size of the gap.

Funded by the European Union

- Overlap: flags whether the element contains an overlap.
- Overlap distance: measures the distance from the element to the overlap.
- Overlap size: quantifies the size of the overlap.

With these variables, we can reconstruct the geometry of each element and the orientation of the layers within the model, allowing for the evaluation of the corresponding surrogate permeability model.

To accomplish this, a Python script has been developed. This script reads the txt file from AddPath containing all the requisite information for each element and retrieves the permeability and macro FVF results. Subsequently, these values are assigned to the lperm file, which is then read by the PAM-RTM software to simulate the RTM process (see Table 2 and Table 3).

In this manner, the AFP simulation software is seamlessly integrated with the RTM simulation software. For a single RTM model, an unlimited number of AFP options can be computed. Furthermore, misalignment, gap, and overlap defects can be addressed by generating meso-scale CFD models to compute the local permeability and FVF of these defects.

Funded by the European Union

4.6 Synthetic Data generation for Defect detection models trainning

During the additive manufacturing process using AFP technology, a point cloud per tape is generated through a profile sensor located in the robot TCP. Using this data is useful not only to detect defects during the deposition process, but also to generate new synthetic data to simulate these defects taking into account the data distribution. Thus, three types of defects can be generated artificially by using Data analytics and AI algorithms in a point cloud: gap between tapes, tape overlap and disalignment between two tapes.

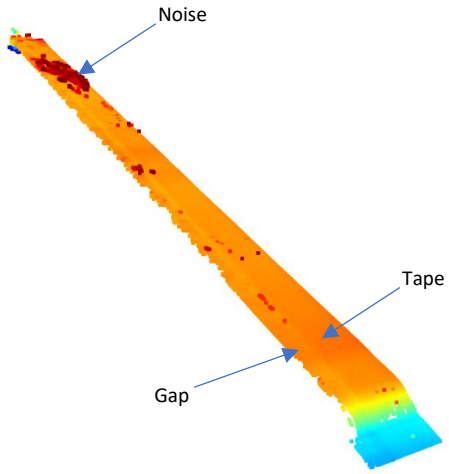

Figure 4.22 Point cloud for a real tape deposition

As it is shown in Figure 4.22, the original point cloud is very noisy, with lots of points out of the main piece in Z coordinate, but it could be quite difficult to see them in 2D. This behaviour is due to the tape material, which is rough, and the failure of the profile sensor when is positioning in Z coordinate in the cloud. To improve the data quality, a cleaning process must be applied to delete all those points that do not belong to the piece itself. To carry out this task, an IQR (interquartile range algorithm) to detect outliers is applied. The result is shown in Figure 4.23.

Funded by the European Union

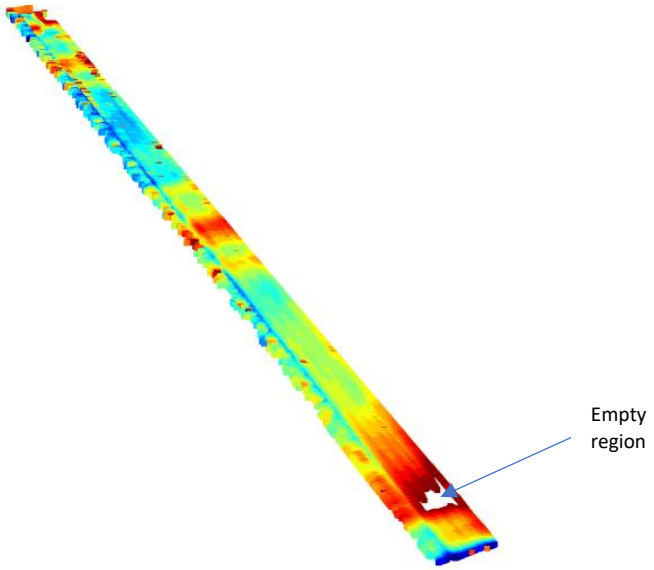

Figure 4.23 Cleaned image by using IQR

Once the point cloud is cleaned, a segmentation process must be applied to separate the gap from the tape. To carry out this task, some clustering algorithms such as DBSCAN were tested but without satisfactory results because there are regions within both surfaces without a sufficient number of points. Again, this is due to poor performance of the profile sensor with these types of rough materials. Finally, a slope detection algorithm was applied to identify two heights (Z coordinate), corresponding to the gap and tape regions, coloured in red and blue in Figure 4.24 respectively. In this case, the gap was established with 5 millimeters width.

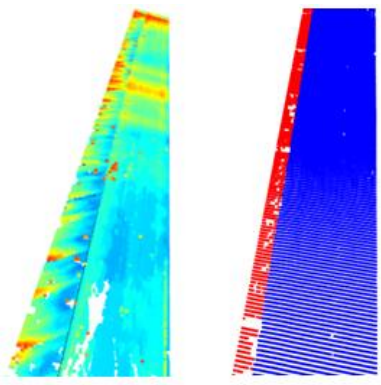

Figure 4.24 Segmented image

Funded by the European Union

Once the gap is segmented, it is possible to create or generate new similar data following the same distribution:

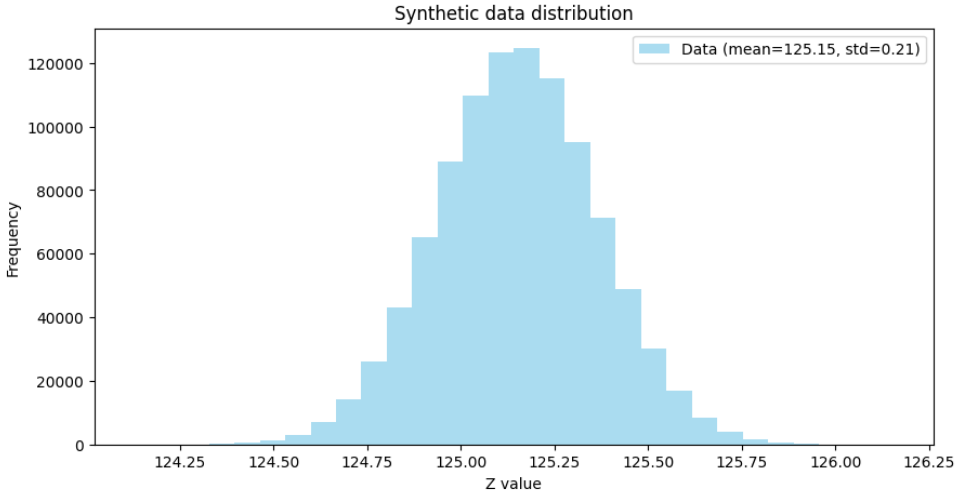

Figure 4.25 Synthetic data distribution

The generation of synthetic data results from this point a straightforward process in which only size parameters must be set into the generative algorithm, such distance between points, desired size of the gap or the tape legth to be generated. By way of illustration, a synthetic defect of a 10 mm gap width was performed by the algorithm, obtaining the following result:

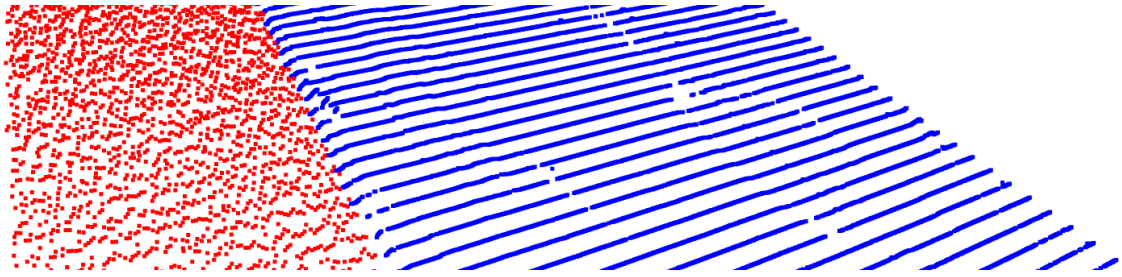

Figure 4.26 Synthetic gap generation

In red colour a synthetic gap is presented, with a 0.1 mm value of distance between points in X coordinate, using the same distribution that the profile sensor detected during the real manufacturing process.

Regarding the misalignment defect type, it occurs when the tape is not perfectly deposed, generating thus a nonparallel tape structure. When the robot applies pressure to depose the

Funded by
the European Union

tape, it is slightly prone to deviation. Visually, this undesired outcome is presented as a non-uniform gap with a different width as length goes increasing as it is shown in Figure 4.27.

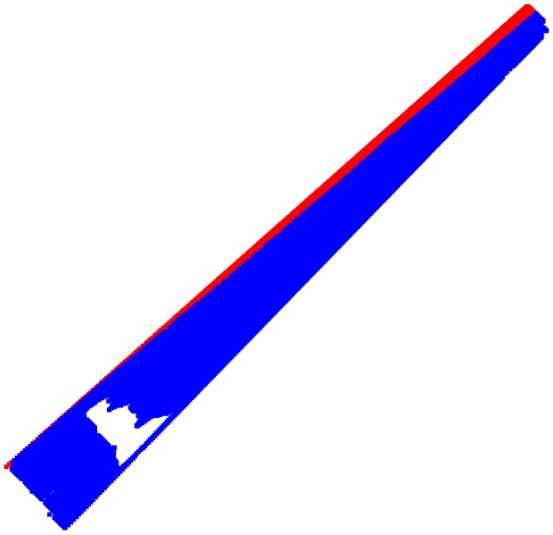

Figure 4.27 Tape misalignment

Apart from the synthetic gap generation with a desired width, now a non-uniform gap generation with a parameterized deviation is available by setting a deviation percentage. Figure 4.28 depicts this deviation tendency along the gap in comparison to the tape. When the deviation is higher than a certain percentage, the gap disappears and two tapes end up stacked, resulting in a new defect; an overlap.

Funded by
the European Union

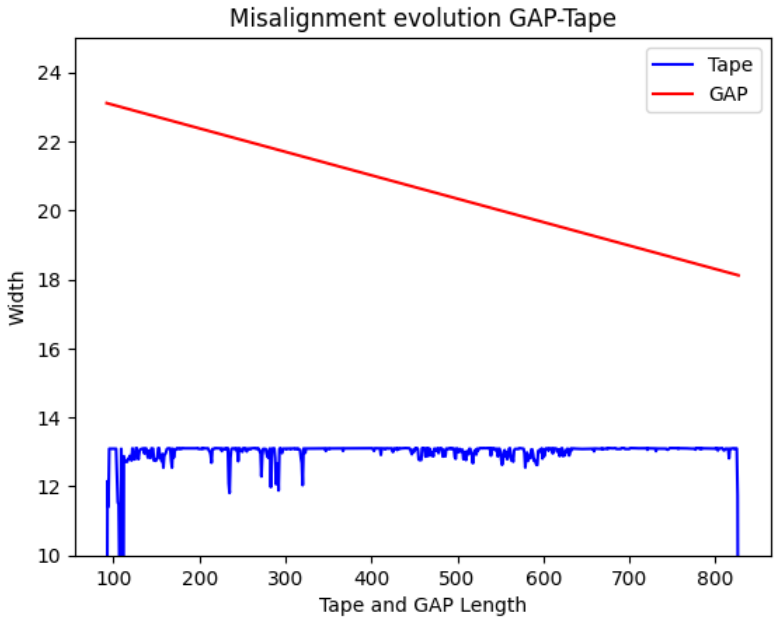

Figure 4.28 Misalignment evolution

Funded by the European Union

5 CONCLUSION AND FUTURE WORK

This report summarizes the progress made in developing simulation capabilities for the AFP and RTM processes, as well as advancements in point cloud data processing for defect analysis. Key achievements include:

1. Integration of defect generation probabilities into the AFP process simulation using ADDPath® and handling of data inflow for simulation.
2. Development of an end-to-end workflow in Python and PyCOMPSs to automate the generation of permeability Reduced Order Models (ROMs) for RTM simulations.
3. Creation of methods to generate synthetic data for gap and misalignment defects based on real data distributions.
4. Preliminary simulations and results showcasing the initial stage leading to final results on the Fan Outlet Guide Vane (FOGV).

Future work will focus on:

1. Integrating experimental defect classification data into the AFP simulation and enhancing the ply definition interface to incorporate ply drop-offs.
2. Completing the training and validation of permeability surrogate models for various defect cases and integrating them into the end-to-end workflow.
3. Exploring additional defect types for synthetic data generation and evaluating the quality and benefits of using synthetic data for defect detection.
4. Conducting refined simulations for each discipline using the generated models to prepare for parametric studies towards the final FOGV design.

The final version of this deliverable, expected in June 2024, will present updated results and conclusions based on the remaining tasks and simulations.